

Novel properties in Josephson junctions involving the $\cos(k_x) \cdot \cos(k_y)$ -pairing state in iron-pnictides

Wei-Feng Tsai,¹ Dao-Xin Yao,¹ B. Andrei Bernevig,² and JiangPing Hu¹

¹*Department of Physics, Purdue University, West Lafayette, IN 47907, USA*

²*Princeton Center for Theoretical Science, Princeton University, Princeton, NJ 08544, USA*

(Dated: October 25, 2018)

We propose a novel trilayer π -junction that takes advantage of the unconventional $s_{x^2y^2} = \cos k_x \cos k_y$ pairing symmetry which changes sign between electron and hole Fermi pockets in the iron-pnictides. In addition, we also present theoretical results for Andreev bound states in thin superconductor-normal metal (or insulator)-iron-pnictide junctions. The presence of non-trivial in-gap states, which uniquely appear in this unconventional pairing state, is a distinct feature in comparison to other singlet pairing states.

A family of iron-based high-temperature superconductors has recently been discovered.¹ These compounds triggered enormous experimental and theoretical interest. In particular, probing the Cooper pair symmetry is critical to understanding the pairing mechanism of this new type of superconductors. Theoretically, many possible gap pairing symmetries have been proposed for iron pnictides, due to the material's multi-orbital nature and complex Fermi surfaces (FSs), with two hole pockets around Γ -point and two electron pockets around M -point [see Fig. 1 (a)].

Among all the candidates, the proposal of s -wave pairing symmetry with relative sign change between hole and electron pockets has appealing advantages.^{2,3,4,5} Two of us have predicted,² based on a local magnetic exchange coupling J_1 - J_2 model,^{6,7,8,9} an unconventional s -wave symmetry with a particular $s_{x^2y^2} = \cos k_x \cos k_y$ form in the reciprocal momentum space. The predicted order parameter is consistent with the relative values of the gap on the hole and electron FSs reported by angle-resolved photo-emission spectroscopy (ARPES) experiments.¹⁰ The proposed symmetry is also consistent with low temperature-dependent penetration depth experiments,^{11,12} and partially explains nuclear spin-lattice relaxation rate.^{13,14} However, since most experiments are only sensitive to the magnitude of the gap of superconducting (SC) order, a direct *phase-sensitive* experiment is essential to map out the complete picture of the pairing symmetry. So far there is no proposed direct phase-sensitive experiment for iron pnictides similar to the dc superconducting quantum interference device (SQUID) interferometer for the cuprates. The difficulty arises from the non-trivial phase structure of the order parameter in k space. One possible phase-sensitive experiment is Andreev spectroscopy in the normal metal to superconductor (NS) junction. Unfortunately, two recent experiments^{15,16} give seemingly conflicting results and detailed theoretical study shows indistinguishable features between an usual s -wave and sign-changed s -wave symmetries.¹⁷

In this paper, we theoretically consider two types of Josephson junctions which have novel properties uniquely associated with a sign-changed s -wave SC order as op-

posed to other (singlet) pairing symmetries. Specifically, the first type of junction we consider is a trilayer SC device where the iron-based superconductor is sandwiched by two other layered, s -wave superconductors [see inset of Fig. 1 (b)]. With certain chosen FSs of the two outside layers which couple stronger, respectively, to the hole and electron pockets of the iron pnictide, due to momentum conservation, it is shown that sign-changed s -wave pairing symmetry uniquely gives rise to a π -junction behavior.^{18,19} The second type is a single-band superconductor-normal metal (or insulator)-iron pnictide (SNS'/SIS') junction (see Fig. 2). Based on the similar physics of Andreev reflection at the interface between a normal metal and a superconductor,^{20,21} we demonstrate that, by adopting a minimal two-orbital model^{2,22} to include the multi-orbital effect and complex FSs, the non-trivial phase structure of the sign-changed s -wave symmetry shows up in the profile of the quasi-particle (QP) local density of states (LDOS) in the normal region of the junction (see Fig. 4): the sign-changed s -wave symmetry state supports in-gap bound state solutions.

Novel π -junction. We propose a composite Josephson junction in which π -junction behavior can occur based on the unusual phase structure of the $s_{x^2y^2}$ -wave pairing. A π -junction defines the situation when the Josephson coupling J between two superconductors becomes *real* and *negative* (with no spontaneous or explicit time reversal symmetry breaking). In other words, the ground state energy (GSE) is minimized as the phase difference Φ between two superconductors is " π ", in contrast to the case of a " 0 "-junction. The occurrence of the π -shift behavior can be usually due to magnetic ordering, strong correlation effects near the tunneling interface,¹⁸ or non-trivial phase structure of the SC order parameter such as $d_{x^2-y^2}$ pairing symmetry.¹⁹

Unlike these common designs, our proposed junction [see the inset of Fig. 1 (b)] is composed of an iron-pnictide (S_m) sandwiched by a top and a bottom quasi-2D s -wave superconductors (S_t and S_b). The interface between any two superconductors is an insulating thin film playing the role of a tunneling barrier. The key requirement for the top and bottom superconducting materials is that *the Cooper-pair tunneling probability is stronger into the*

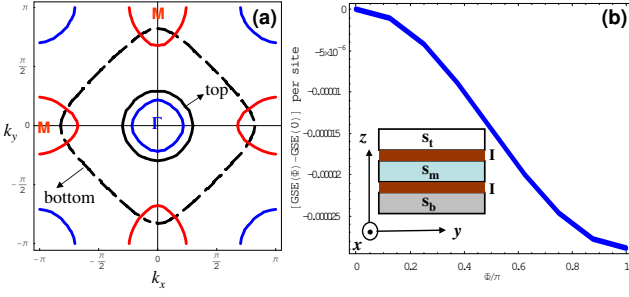


FIG. 1: (Color online) The plots of (a) schematic stacked Fermi surfaces from tri-layer superconducting junction and (b) the ground state energy deviation (from $\Phi = 0$ case) per site as a function of relative phase Φ with $\theta_m = 0$. The colored curves in (a) represent the FSs of the iron-pnictides.

hole (electron) pockets for the top (bottom) or vice versa. This could be engineered to be due to the normal state FSs of the top and bottom superconductors. One possible way to achieve this condition is to select a small FS and a large FS around Γ point for the top layer and the bottom layer, respectively [see Fig. 1 (a)], provided the in-plane (perpendicular to the tunneling direction) momentum is conserved ideally after tunneling.

A simple mean-field model Hamiltonian for this tri-layer junction can be of the form, $H_J = H_t + H_m + H_b + H_T$, where $H_\eta = \sum_{\mathbf{k}} \hat{\psi}_\eta^\dagger [(\varepsilon_{\eta,\mathbf{k}} - \mu)\sigma_3 + \Delta_\eta e^{i\theta_\eta} \sigma_+ + \Delta_\eta e^{-i\theta_\eta} \sigma_-] \hat{\psi}_\eta$ for $\eta = t, b$. $\varepsilon_{\eta,\mathbf{k}}$ has the form of $-2t_\eta(\cos k_x + \cos k_y) + \varepsilon_\eta$, $\sigma_\pm = (\sigma_1 \pm i\sigma_2)/2$, and $\hat{\psi}_\eta$ is the usual Nambu spinor, $\hat{\psi}_\eta^\dagger = (c_{\eta,\mathbf{k},\uparrow}^\dagger, c_{\eta,-\mathbf{k},\downarrow})$. The difference between the top and bottom SC phases is gauge invariant for the whole junction and is set to be $\Phi = \theta_t - \theta_b$. H_m , the Hamiltonian of the iron pnictide, is shown in Eq. (5) transformed into momentum space with band parameters and non-vanishing $\Delta_{s2} = \Delta e^{i\theta_m}$ given in the caption of Fig. 3. The tunneling Hamiltonian, H_T , which connects neighboring layers, takes the simple form: $H_T = \sum_{\mathbf{p},\mathbf{k},\eta} \hat{\psi}_\eta^\dagger(\mathbf{p}) \hat{h}_{T,\eta} \hat{\psi}_m(\mathbf{k})$, where $\hat{h}_{T,\eta}$ is a 2×4 matrix,

$$\begin{pmatrix} g_\eta & 0 & g_\eta & 0 \\ 0 & -g_\eta & 0 & -g_\eta \end{pmatrix} \delta_{\mathbf{p},\mathbf{k}} \quad (1)$$

and the spinor $\hat{\psi}_m^\dagger = (c_{1,\mathbf{k},\uparrow}^\dagger, c_{1,-\mathbf{k},\downarrow}, c_{2,\mathbf{k},\uparrow}^\dagger, c_{2,-\mathbf{k},\downarrow})$ describes the iron pnictide. Note that we have assumed that the dispersion along z -axis is irrelevant and negligible in quasi-2D materials.

For demonstration purpose, we choose parameters $t_t = t_b = 1$, $\varepsilon_t = 4.78$, $\varepsilon_b = 1.88$, $g_t = g_b = 0.01$, $\Delta_t = 0.5$, $\Delta_b = 0.4$, $\Delta = 0.5$, and $\theta_m = 0$. The stacked FSs in the first Brillouin zone from each layer is shown in Fig. 1 (a). Now, it is easy to diagonalize H_J and the ground-state energy for this mean-field Hamiltonian is simply the sum of all QP eigen-energies below $E = 0$. As presented in Fig. 1 (b), the ground state energy per

site relative to the energy of $\Phi = 0$ decreases as a function of Φ with its minimum located at “ π ”. The physics of this result can be easily captured by the perturbation calculations of GSE, which give, up to second order of g_η^2 , $-J_{tm} \cos(\theta_t - \theta_m) - J_{mb} \cos(\theta_m - \theta_b)$, where the Josephson couplings, $J_{tm} > 0$, $J_{mb} < 0$ (the sign difference between the Josephson couplings is due to π phase difference between electron-like and hole-like FSs), have similar form of the textbook derivation.²³ It is obvious to see that the global minimum reaches at $|\theta_t - \theta_b| = \pi$. The overall junction shows “ π ” behavior.

Some comments on the experimental realization are in order. First, “large” or “small” FS is meaningful only when the lattice constant a is equal or comparable to the iron pnictides, where the nearest-neighbor Fe-Fe distance is around 2.85\AA . Second, to make the tunneling processes reasonably dominated by in-plane momentum conservation, quasi-2D, s -wave SC materials should be used for the top and bottom layers due to their irrelevant dispersion along z direction and the epitaxial growing technique may be useful for making the coherent-tunnel interfaces. Based on these considerations, some plausible candidates for the large FS are, for instance, MgB_2 from its π band with $a \sim 3\text{\AA}$ or thin film of Beryllium with $a \sim 2.3\text{\AA}$; for the small FS, it could be 2H-NbSe_2 , where $a \sim 3.45\text{\AA}$.²⁴

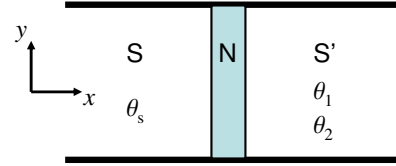


FIG. 2: (Color online) A schematic plot of the SNS' junction.

SNS'/SIS' junctions. A further feature of the $s_{x^2y^2}$ -SC is revealed by considering a Josephson junction which connects, on one side, a single-band s -wave superconductor, through a normal metal to, on the other side, an iron-based superconductor.²⁵ We assume its QP spectrum is well approximated by a BCS type mean-field Hamiltonian subject to an inhomogeneous pairing field along the tunneling direction. Ignoring the z -axis for simplicity, the 2D model Hamiltonian of this junction reads,

$$\mathcal{H} = \Theta(-x - \frac{d}{2})H_S + \Theta(\frac{d}{2} - |x|)H_N + \Theta(x - \frac{d}{2})H_{S'} + H_T, \quad (2)$$

$$H_S = -t_S \sum_{\langle \mathbf{r}\mathbf{r}' \rangle, \sigma} c_{\mathbf{r},\sigma}^\dagger c_{\mathbf{r}',\sigma} - \tilde{\mu} \sum_{\mathbf{r},\sigma} c_{\mathbf{r},\sigma}^\dagger c_{\mathbf{r},\sigma} + \sum_{\mathbf{r}} (\Delta_s c_{\mathbf{r},\uparrow}^\dagger c_{\mathbf{r},\downarrow}^\dagger + h.c.), \quad (3)$$

$$H_N = -t_N \sum_{\langle \mathbf{r}\mathbf{r}' \rangle, \sigma} f_{\mathbf{r},\sigma}^\dagger f_{\mathbf{r}',\sigma} + (U - \tilde{\mu}) \sum_{\mathbf{r},\sigma} f_{\mathbf{r},\sigma}^\dagger f_{\mathbf{r},\sigma}, \quad (4)$$

where $\Theta(x)$ is the Heaviside function, the shifted chemical potential, $\tilde{\mu} = \mu - \epsilon$, guarantees a partially filled

band, and U denotes barrier potential. To mimic the iron pnictide FS, we adopt a two-orbital exchange coupling model.² This leads to a somewhat complicated form of $H_{S'} = H_0 + H_\Delta$, where we separate it into the band structure and pairing field parts,

$$\begin{aligned}
H_0 &= \sum_{\mathbf{r},\sigma} [-t_1 c_{1,\mathbf{r},\sigma}^\dagger c_{1,\mathbf{r}+\hat{x},\sigma} - t_2 c_{1,\mathbf{r},\sigma}^\dagger c_{1,\mathbf{r}+\hat{y},\sigma} + h.c.] \\
&+ \sum_{\mathbf{r},\sigma} [-t_2 c_{2,\mathbf{r},\sigma}^\dagger c_{2,\mathbf{r}+\hat{x},\sigma} - t_1 c_{2,\mathbf{r},\sigma}^\dagger c_{2,\mathbf{r}+\hat{y},\sigma} + h.c.] \\
&+ \sum_{\langle\langle\mathbf{r}\mathbf{r}'\rangle\rangle} \sum_{\alpha,\sigma} -t_3 c_{\alpha,\mathbf{r},\sigma}^\dagger c_{\alpha,\mathbf{r}',\sigma} - \mu \sum_{\alpha,\mathbf{r},\sigma} c_{\alpha,\mathbf{r},\sigma}^\dagger c_{\alpha,\mathbf{r},\sigma} \\
&- \sum_{\langle\langle\mathbf{r}\mathbf{r}'\rangle\rangle} \sum_{\sigma} [t_4 e^{i\frac{\pi}{2}[(x'-x)+(y'-y)]} c_{1,\mathbf{r},\sigma}^\dagger c_{2,\mathbf{r}',\sigma} + h.c.], \\
H_\Delta &= [\sum_{\alpha,\mathbf{r}} \Delta_0 c_{\alpha,\mathbf{r},\uparrow}^\dagger c_{\alpha,\mathbf{r},\downarrow}^\dagger + \sum_{\alpha,\langle\langle\mathbf{r}\mathbf{r}'\rangle\rangle} \frac{\Delta_{s2}}{4} c_{\alpha,\mathbf{r},\uparrow}^\dagger c_{\alpha,\mathbf{r}',\downarrow}^\dagger \\
&+ \sum_{\alpha,\langle\langle\mathbf{r}\mathbf{r}'\rangle\rangle} \frac{\Delta_d e^{i\pi(\alpha-1)}}{4} \phi_{\mathbf{r}\mathbf{r}'} (c_{\alpha,\mathbf{r},\uparrow}^\dagger c_{\alpha,\mathbf{r}',\downarrow}^\dagger - c_{\alpha,\mathbf{r},\downarrow}^\dagger c_{\alpha,\mathbf{r}',\uparrow}^\dagger) \\
&+ \sum_{\alpha,\langle\langle\mathbf{r}\mathbf{r}'\rangle\rangle} \frac{\Delta_{s1}}{4} (c_{\alpha,\mathbf{r},\uparrow}^\dagger c_{\alpha,\mathbf{r}',\downarrow}^\dagger - c_{\alpha,\mathbf{r},\downarrow}^\dagger c_{\alpha,\mathbf{r}',\uparrow}^\dagger)] + h.c. \quad (5)
\end{aligned}$$

where $\alpha = 1, 2$ correspond to d_{xz} and d_{yz} orbitals, respectively, and the hopping parameters are given in Fig. 3. $\langle\langle\mathbf{r}\mathbf{r}'\rangle\rangle$ represents a next nearest-neighbor pair and $\phi_{\mathbf{r}\mathbf{r}'} = 1(-1)$ as $\mathbf{r} - \mathbf{r}' = \pm\hat{x}(\hat{y})$. All pairing fields considered in \mathcal{H} are set to be real.²⁶ $\Delta_0, \Delta_{s1}, \Delta_{s2}$, and Δ_d correspond to intra-orbital on-site, $\cos k_x + \cos k_y$, $\cos k_x \cos k_y$, and $\cos k_x - \cos k_y$ pairing strength, respectively, and inter-orbital pairing is ignored due to its small contribution as discussed in Ref. 2. Finally, H_T describes the tunneling amplitudes across two interfaces around $\pm d/2$. It can be written as

$$H_T = g_S \sum_{\sigma} c_{\mathbf{r}_L,\sigma}^\dagger f_{\mathbf{r}'_L,\sigma} + g_{S'} \sum_{\alpha,\sigma} c_{\alpha,\mathbf{r}_R,\sigma}^\dagger f_{\mathbf{r}'_R,\sigma} + h.c., \quad (6)$$

where $\mathbf{r}_L, \mathbf{r}'_L$ ($\mathbf{r}_R, \mathbf{r}'_R$) are understood to be coordinates across the left (right) interface.

Before proceeding to compute the QP spectrum and the corresponding LDOS, it is important to realize that \mathcal{H} is particle-hole symmetric under $c_{\mathbf{r},\uparrow} \rightarrow c_{\mathbf{r},\downarrow}^\dagger, c_{\mathbf{r},\downarrow} \rightarrow -c_{\mathbf{r},\uparrow}^\dagger$ (for all fermion operators), and hence its spectrum should be symmetric with respect to zero-energy. Taking advantage of the translational symmetry transverse to the tunneling direction x , \mathcal{H} can be further decomposed into a sum of 1D Hamiltonians by partially Fourier-transforming along (100) surface (y direction). As a consequence, the whole system is mapped onto an 1D effective lattice in the form of $\mathcal{H} = \sum_{k_y} H_{1D}(k_y)$. Basically, this transformation results in effective chemical potential and pairing fields with k_y -dependence.

We diagonalize the model Hamiltonian $H_{1D}(k_y)$ for $-\pi \leq k_y < \pi$ on the Nambu basis Ψ , where in numerical calculations we take the total number of the 1D lattice

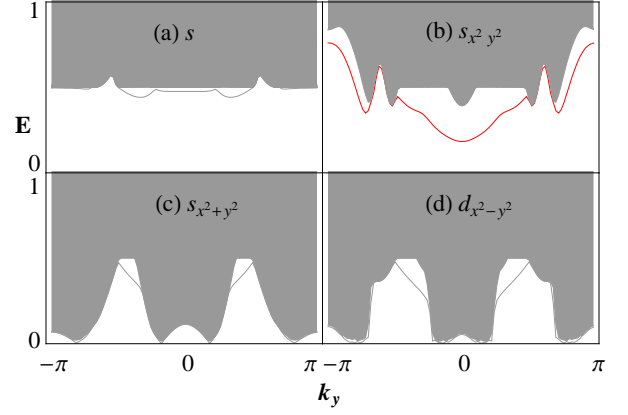


FIG. 3: (Color online) QP spectrum in the SNS' junction involving the iron-pnictide with various pairing symmetries. The red line represents Andreev bound states in the case of $s_{x^2y^2}$ -wave pairing. The used parameters are $U = 0$, $\tilde{\mu} = -2$, $\Delta_s = 0.5$, $g_S = g_{S'} = 1$, $t_1 = -1$, $t_2 = 1.3$, $t_3 = -0.85$, $t_4 = -0.85$, $\mu = 1.58$, $n_m = 1$, and the pairing strength is, respectively, (a) $\Delta_0 = 0.5$ ($n=201$), (b) $\Delta_{s2} = 0.5$ ($n=201$), (c) $\Delta_{s1} = 0.5$ ($n=201$), and (d) $\Delta_d = 0.5$ ($n=601$) in energy units, $t_s \equiv 1$.

sites n sufficiently large with open boundary conditions; the normal metal is always set in the middle of system and it is n_m -site wide. This length is always much less than the SC coherence length. In Fig. 3, we show numerical results of the zero temperature QP spectrum as a function of k_y for various pairing symmetries of the iron-pnictides at $\mu = 1.58$ (electron doped). In addition, to visualize the Andreev bound states, in Fig. 4 we also compute each corresponding QP-LDOS as a function of position and energy, $D(x, \omega) = \sum_{k_y, i} |\Psi_i(x, k_y)|^2 \delta(\omega - \epsilon_i)$, where i denotes the i th eigenfunction. The magnitude of the bulk SC order parameters on both sides of the junction is taken to be the same. The ratio of the gap to the half band-width of the spectrum is around 0.02 and the coherence length is estimated as $\xi \sim v_F/\Delta_s \sim 4a$.

As clearly seen in Fig. 3, the presence of the in-gap Andreev bound states with significant weight in different k_y channels for the extended s -wave $\cos k_x \cos k_y$ ($s_{x^2y^2}$) pairing symmetry is a sharp feature distinguishing it from other pairing symmetries. Although in addition to (gray-color filled) continuum states there are discrete energy levels for s , $s_{x^2+y^2}$, and $d_{x^2-y^2}$ pairing symmetries, they are either near the maximum gap edge (s) or only appear in certain range of k_y (for $s_{x^2+y^2}$, $d_{x^2-y^2}$). Especially for the latter case, due to the presence of nodal points on the electron or the hole pockets, the contribution from scattering-state can easily overwhelm that from the bound states and can lead to qualitatively different QP-LDOS from the case of $s_{x^2y^2}$ -wave, where a sharp peak appears at the positive subgap energy.

Furthermore, two observations deserve mentioning. First, the features shown in Figs. 3 and 4 do not change

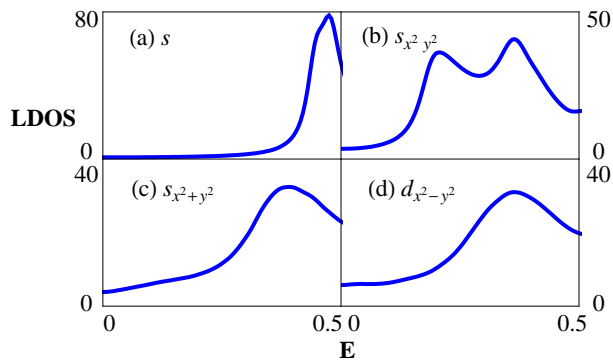


FIG. 4: (Color online) QP-LDOS at $x = 0$ in the SNS' junction involving iron-pnictide with various pairing symmetries. The used parameters are the same as in drawing Fig. 3, except that $n = 121$ for (a)-(c) and $n = 161$ for (d).

much for different doping levels as long as the doping concentration is not large enough so that the Fermi surfaces pass the nodal line of $\cos k_x \cos k_y$, i.e., $k_x = \pm\pi/2$ and $k_y = \pm\pi/2$. Second, if the barrier potential U is greater than the difference between μ and the band bottom, the normal region becomes insulating. This moves the subgap peak in the $s_{x^2y^2}$ LDOS closer to the gap edge without destroying it.

Can we understand the presence of such non-trivial bound states for the $s_{x^2y^2}$ -wave pairing in a simple way? A physical insight for this junction involving such an unconventional symmetry can be obtained by treating the *bands* at the electron and hole pockets in the iron-pnictide as independent of each other.²⁷ Consequently, a simple description for the junction based on Bogoliubov-De Gennes (BdG) equations reads:

$$[\hat{H}_{0,\lambda}\sigma_3 + \Delta_\lambda(\mathbf{r})\sigma_+ + \Delta_\lambda^*(\mathbf{r})\sigma_-]\psi(\mathbf{r}) = \epsilon_\lambda\psi(\mathbf{r}), \quad (7)$$

where $\lambda = 1, 2$ are the *band* indices, and σ_i ($i = 1, 2, 3$) are the Pauli matrices with $\sigma_\pm = (\sigma_1 \pm i\sigma_2)/2$ acting in the Nambu space, $\psi = [\tilde{u}_\lambda(\mathbf{r}), \tilde{v}_\lambda(\mathbf{r})]^t$. $\hat{H}_{0,\lambda}$ contains the band information of non-interacting electrons

and $\Delta_\lambda(\mathbf{r})$ corresponds to the pairing field in the same band λ . Along the tunneling direction x , the inhomogeneous $\Delta_\lambda(\mathbf{r})$ is modeled by $\Delta_\lambda(x) = \Delta_s e^{i\theta_s}$ as $x < 0$ and $\Delta_\lambda(x) = \Delta_\lambda e^{i\theta_\lambda}$ as $x > 0$. For simplicity, we set $\theta_s = 0$ hereafter and keep in mind that for the sign-changed s -wave symmetry, $\theta_1 = \theta_2 + \pi$. For electrons near FSs, it is valid to linearize BdG equations within WKJB approximation, $\psi \sim e^{i\mathbf{k}_F \cdot \mathbf{r}} \phi(\mathbf{r})$, $\phi(\mathbf{r}) = (u(\mathbf{r}), v(\mathbf{r}))^t$ and then the BdG equations are now reduced to the form of 1D Dirac equation if we further take the advantage of translational symmetry in transverse direction,

$$[-iv_{Fx}\partial_x\sigma_3 + \Delta_\lambda(x)\sigma_+ + \Delta_\lambda^*(x)\sigma_-]\phi(x) = \epsilon_\lambda\phi(x). \quad (8)$$

After straightforward calculations with trial bound state solutions, $u(v) \sim u_0(v_0)e^{-\gamma \pm x}$, as studied in Ref. 27, the discrete energy level within the gap is given by $E_0 = \pm(\Delta_s\Delta_\lambda \sin\theta_\lambda)/\sqrt{\Delta_s^2 + \Delta_\lambda^2 - 2\cos\theta_\lambda\Delta_s\Delta_\lambda}$, provided $\cos\theta_\lambda < \min(\Delta_\lambda/\Delta_s, \Delta_s/\Delta_\lambda)$. The pair of solutions with eigenvalues symmetric with respect to zero-energy follows from the particle-hole symmetry of the BdG equations. It is clear to see that when superconductors on both sides of the junction are in phase ($\theta_\lambda = 0$) no bound state solution is found, while when they are out of phase ($\theta_\lambda = \pi$) there are doubly-degenerate zero modes.²⁷

The significance of this simple result is that as long as $\theta_1 = 0$ (or $\theta_2 = 0$), there are always zero modes trapped in the normal region of the junction involving iron pnictides with sign-changed s -wave pairing symmetry. However, in a more realistic system with band structure such as our SNS' junction it usually introduces finite effective mass for the band electrons, which destroys the validity of using linearized Eq. (8) (where the effective mass goes to infinity). As a result, the to-be-degenerate zero modes split²⁸ as we see in Fig. 3 (only $E > 0$ shown). The same argument is also applicable when we further consider the effect brought by k_y in our $H_{1D}(k_y)$.

Acknowledgements. We thank E. Berg and C. Fang for stimulating and useful discussions. JPH and WFT are supported by NSF Grant No. PHY-0603759 and DXY is supported by NSF Grand No. DMR-0804748.

¹ Y. Kamihara *et al.*, J. Am. Chem. Soc. **130**, 3296 (2008).
² K. Seo, B. A. Bernevig, and J. Hu, Phys. Rev. Lett. **101**, 206404 (2008).
³ I. I. Mazin *et al.*, Phys. Rev. Lett. **101**, 057003 (2008).
⁴ F. Wang *et al.*, Phys. Rev. Lett. **102**, 047005 (2009) and references therein.
⁵ V. Cvetkovic and Z. Tesanovic, Europhys. Lett. **85**, 37002 (2009).
⁶ T. Yildirim, Phys. Rev. Lett. **101**, 057010 (2008).
⁷ F. Ma Z.-Y. Lu, and T. Xiang, Phys. Rev. B **78**, 224517 (2008).
⁸ Q. Si and E. Abrahams, Phys. Rev. Lett. **101**, 076401 (2008).

⁹ C. Fang *et al.*, Phys. Rev. B **77**, 224509 (2008).
¹⁰ H. Ding *et al.*, Europhys. Lett. **83**, 47001 (2008); L. Wray *et al.*, Phys. Rev. B **78**, 184508 (2008); L. Zhao *et al.*, Chin. Phys. Lett. **25**, 4402 (2008).
¹¹ C. Martin *et al.*, arXiv:0807.0876.
¹² K. Hashimoto *et al.*, Phys. Rev. Lett. **102**, 017002 (2009).
¹³ M. M. Parish, J. Hu, and B. A. Bernevig, Phys. Rev. B **78**, 144514 (2008).
¹⁴ K. Matano *et al.*, Europhys. Lett. **83**, 57001 (2008); H.-J. Grafe *et al.*, Phys. Rev. Lett. **101**, 047003 (2008); Y. Nakai *et al.*, J. Phys. Soc. Jpn. **77**, 073701 (2008).
¹⁵ T. Y. Chen *et al.*, Nature **453**, 1224 (2008).
¹⁶ L. Shan *et al.*, Europhys. Lett. **83**, 57004 (2008).

- ¹⁷ J. Linder and A. Sudbo, Phys. Rev. B **79**, 020501(R) (2009).
- ¹⁸ See E. Berg, E. Fradkin, and S. A. Kivelson, Phys. Rev. B **79**, 064515 (2009) and references therein.
- ¹⁹ D. J. Van Harlingen, Rev. Mod. Phys. **67**, 515 (1995).
- ²⁰ C.-R. Hu, Phys. Rev. Lett. **72**, 1526 (1994); S. Kashiwaya and Y. Tanaka, Rep. Prog. Phys. **72**, 1641 (2000), and references therein.
- ²¹ P. Ghaemi, F. Wang, and A. Vishwanath, Phys. Rev. Lett. **102**, 157002 (2009).
- ²² S. Raghunathan *et al.*, Phys. Rev. B **77**, 220503(R) (2008).
- ²³ P. G. de Gennes, *Superconductivity of Metals and Alloys* (Addison-Wesley, New York, 1989).
- ²⁴ For instance, see J. Kortus *et al.*, Phys. Rev. Lett. **86**, 4656 (2001); A. E. Curzon *et al.*, J. Phys. C **2** 382 (1969); T. Yokoyama *et al.*, Science **294**, 2518 (2001).
- ²⁵ Using a similar SNS' junction, $0-\pi$ oscillations in the Josephson current have been found by J. Linder, I. B. Sperstad, and A. Sudbo, Phys. Rev. B **80**, 020503(R) (2009).
- ²⁶ We neglect the possibility of a spontaneously time reversal symmetry broken ground state.
- ²⁷ T. K. Ng and N. Nagaosa, arXiv:0809.3343.
- ²⁸ W.-F. Tsai *et al.*, unpublished note.